Available online at www.sciencedirect.com
ScienceDirect
Polymer 47 (2006) 7935–7942
polymer
www.elsevier.com/locate/polymer

Non-isothermal elimination process in the solid state of *n*-alkyl-sulphinyl precursor polymers towards conjugated poly[2-(3′,7′-dimethyloctyloxy)-5-methoxy-1,4-phenylene vinylene] studied with MTDSC and TGA

E. Kesters [a], S. Swier [b], G. Van Assche [b], L. Lutsen [c], D. Vanderzande [a,c], B. Van Mele [b,*]

[a] *IMO, Division Chemistry, Campus Diepenbeek, Universiteit Hasselt, Agoralaan Building D, B-3590 Diepenbeek, Belgium*
[b] *Vrije Universiteit Brussel (VUB), Department of Physical Chemistry and Polymer Science, Pleinlaan 2, 1050 Brussel, Belgium*
[c] *IMEC, Division IMOMEC, Wetenschapspark 1, 3590 Diepenbeek, Belgium*

Received 21 March 2006; received in revised form 29 August 2006; accepted 5 September 2006
Available online 2 October 2006

Abstract

The elimination process of *n*-alkyl-sulphinyl precursor polymers towards conjugated poly[2-(3′,7′-dimethyloctyloxy)-5-methoxy-1,4-phenylene vinylene], or OC_1C_{10}-PPV, was studied with modulated temperature differential scanning calorimetry (MTDSC) and thermogravimetric analysis (TGA), with a focus on the subsequent reactions of the elimination products. The latter reactions were monitored using the non-reversing heat flow and the heat capacity (C_p) measured in non-isothermal MTDSC experiments. The disproportionation reaction occurs in a temperature range between 85 and 135 °C and is seen as an increase in C_p. Water and elimination products released during the elimination reaction act as plasticizers and lower the T_g. TGA experiments show that the temperature, film thickness, and the eliminated group play an important role on the diffusion and evaporation of the elimination products. The elimination products can further decompose and interact with the conjugated system to form undesirable crosslinks (network formation) in a temperature range of 140–160 °C.

Keywords: Conjugated polymers; Poly(*p*-phenylene vinylene); Elimination reaction

1. Introduction

The microstructure of conjugated polymers is of major importance for their performance in the final applications, e.g. the quality and morphology of the conjugated system strongly affect the performance of the material in polymeric light emitting diodes (PLED). In the case of precursor systems, the conversion from the precursor to the conjugated polymer may influence both properties. A large number of papers deal with the conversion of sulphonium poly(*p*-phenylene vinylene) (PPV) precursor polymers [1]. The broad range of elimination conditions that are defined in these reports, however, underlines the difficulty of monitoring the conversion process. The conjugated polymer that is studied here is poly[2-(3′,7′-dimethyloctyloxy)-5-methoxy-1,4-phenylene vinylene], or OC_1C_{10}-PPV. It is a typical example of a material that is soluble in its conjugated form [2–6]. The most used synthetic route to prepare the OC_1C_{10}-PPV conjugated polymer is the direct ''Gilch route'', a one-step synthesis in basic environment [7]. Another promising synthetic route to prepare the conjugated OC_1C_{10}-PPV polymer is a non-ionic precursor route developed by Vanderzande et al., the ''sulphinyl route'' [8–11].

In the last years, a lot of research has been done on the OC_1C_{10}-PPV type of polymers, because of their relatively easy synthesis, their good processing capabilities into single-layer

* Corresponding author. Tel.: +32 2 6293276; fax: +32 2 6293278.
E-mail addresses: kesterse@imec.be (E. Kesters), steven.swier@dowcorning.com (S. Swier), gvassche@vub.ac.be (G. Van Assche), laurence.lutsen@uhasselt.be (L. Lutsen), dirk.vanderzande@uhasselt.be (D. Vanderzande), bvmele@vub.ac.be (B. Van Mele).

0032-3861/$ - see front matter © 2006 Elsevier Ltd. All rights reserved.
doi:10.1016/j.polymer.2006.09.018

devices, and their high luminescence yields [12]. Recently promising results were also obtained for its use in photovoltaic (solar) cells [13–16]. Therefore, OC_1C_{10}-PPV has become a standard electroluminescent material inside the PLED and plastic solar cell research. An important disadvantage of such materials, however, is that in some cases it is difficult to develop the multilayer structures that are required for highly efficient LEDs, since co-solubility of the different materials is hard to avoid. Solid state elimination from a precursor polymer film may be desirable in those applications where the deposition of conjugated PPV from solution is impossible. In such a case, the precursor polymer film can be deposited from other solvents (avoiding co-solubility). Moreover, solid state elimination facilitates using non-soluble PPV variants.

The aim of this work is to obtain information about all reactions and phenomena that occur during the elimination from precursor polymer to the conjugated polymer, in both solid state and solution. From previous in situ non-isothermal FT-IR and UV–vis experiments it was clear that the elimination reaction starts at around 70 °C in nitrogen flow [17]. However, the latter techniques do not provide information about the subsequent reactions of the elimination products. For this purpose, FT-IR and UV–vis spectroscopy, modulated temperature differential scanning calorimetry (MTDSC), and thermogravimetric analysis (TGA) will be used as in situ analytical techniques, each examining a typical reaction or part of the conversion process. The study in solid state may enable us to observe in more detail the subsequent reactions of the elimination products occurring during thermal conversion. This insight is not only relevant to evaluate the conditions in which conversion can be performed in solid state, but can relate also to side reactions occurring on conversion in liquid state. In this way this work has in fact contributed to the development of conversion procedures in liquid state to obtain conjugated materials with extremely low structural defect levels [18].

2. Experimental section

2.1. Analytical techniques and sample preparation

Modulated temperature differential scanning calorimetry (MTDSC) measurements were performed on a TA Instruments 2920 Modulated DSC with MTDSC option and a Refrigerated Cooling System. Helium was used as a purge gas (25 mL/min). Indium and cyclohexane were used for temperature calibration; the former was also used for enthalpy calibration. Heat capacity calibration was performed with a poly(methylmethacrylate) standard (PMMA), supplied by Acros. The heat capacity difference between 150 and 80 °C (above and below the T_g) is used to calibrate the heat capacity changes measured. The ratio of the heat capacity difference obtained from literature [19] over the measured difference gives the calibration factor K_{C_p}.

The non-isothermal experiments in solid state are performed in high-pressure stainless steel pans (HPS) at a heating rate of 2.5 °C/min. The superimposed sinusoidal temperature program (=temperature modulation) for HPS pans was ±0.5 °C (amplitude) per 60 s (period), which is notated as 0.5 °C/100 s. The sample mass is between 10 and 15 mg. For the solid state MTDSC experiments, films of precursor polymer and conjugated polymer with a thickness of 500 μm are pressed at 35 °C between aluminium foils. Reproducible MTDSC measurements were carried out using this method of sample preparation. Each HPS pan is hermetically sealed, to avoid evaporation of elimination products. Some non-isothermal measurements are carried out with a LNCA (Liquid Nitrogen Cooling Accessory) cooling system to reach temperatures down to −150 °C.

A TGA 2950 ThermoGravimetric Analyser from TA Instruments is used to measure weight losses. Step-wise isothermal experiments at 85, 100, 140, and finally at 200 °C are carried out under a constant flow of an inert nitrogen atmosphere. The TGA pan is first weighed and afterwards a mixture of 5% (m/m) polymer/$CHCl_3$ is sprayed on the bottom of the TGA pan. A polymer film is obtained by evaporation of $CHCl_3$. A second layer is applied using the same method. Then, the pan is placed in a vacuum oven during 2–3 h at 10^{-2} mmHg and 25 °C to make sure that all $CHCl_3$ has evaporated. Using this method, uniform films with different thicknesses can be obtained.

^{1}H NMR spectra were obtained in $CDCl_3$ at 300 MHz on a Varian Inova Spectrometer using a 5 mm probe. Chemical shifts (δ) in ppm were determined relative to the residual $CHCl_3$ resonance shift (7.24 ppm). The ^{13}C NMR experiments were recorded at 75 MHz on the same spectrometer using a 5 mm broadband probe. Chemical shifts were defined relative to the ^{13}C resonance shift of $CHCl_3$ (77.0 ppm).

2.2. Materials

n-Alkyl-sulphinyl OC_1C_{10}-PPV precursor polymers and the OC_1C_{10}-PPV conjugated polymer (without elimination products): the synthesis and characterisation of these polymers are described in literature [20].

n-Butyldisulphide: this product is commercially available (Acros). ^{1}H NMR ($CDCl_3$, 400 MHz): δ 0.89 (t, 6H, CH_3), 1.37 (qui, 4H, $CH_3(CH_2)_3$), 1.63 (qui, 4H, CH_2CH_2S), 2.65 (t, 4H, CH_2S) ppm; IR (KBr): 2871 ν (CH_2 symm.), 1463 ν (CH_2–S deformation), 1268 ν (CH_2–S wag), 1216 ν (CH_2 twist) cm^{-1}; DIP-MS (EI, *m*/*z*, rel. int.): 178 ($[M]^+$, 40), 121 ($[M-C_4H_9]^+$, 30), 87 ($[M-SC_4H_9]^+$, 5), 57 ($C_4H_9^+$, 100).

n-Butyl-thiosulphinate [21,22]: a solution of *m*-CPBA (5.61 mmol, 1.17 g) in dichloromethane (10 mL) was added to a solution of *n*-butyldisulphide (1.00 g, 5.61 mmol) in dichloromethane (100 mL) and cooled in an ice-water bath. After stirring for 1 h at 0 °C and 2 h at ambient temperature, water (200 mL) was added. The organic layer was extracted with water (3 × 200 mL) and aqueous $NaHCO_3$ (sat.) (2 × 150 mL), dried with anhydrous magnesium sulphate and concentrated in vacuum. After purification by column chromatography on silica using chloroform as eluent, *n*-butyl-thiosulphinate was collected as a colourless oil (0.76 g, 70%). ^{1}H NMR ($CDCl_3$, 400 MHz): δ 0.86 (t, 6H, CH_3),

1.78 (m, 4H, $CH_2CH_2S(O)SCH_2CH_2$), 3.1 (m, 4H, $CH_2S(O)SCH_2$) ppm; ^{13}C NMR ($CDCl_3$, 100 MHz): δ 13.9 (CH_3), 30.7 ($CH_2CH_2SS(O)$), 31.59 ($CH_2CH_2S(O)S$), 32.62 ($CH_2SS(O)$), 55.98 (CH_2–S(O)S); IR (KBr): 2956, 2925 ν (CH_2 asymm.), 2871 ν (CH_2 symm.), 1462 ν (CH_2–S deformation), 1082 ν (S(O)) cm^{-1}.

n-Butyl-thiosulphonate: a solution of *n*-butanethiol (0.6 g, 5.55 mmol) and Na*t*-BuO (0.53 g, 5.55 mmol) in THF (25 mL) was added to a solution of *n*-butanesulphonyl chloride (0.87 g, 5.55 mmol) in tetrahydrofuran (THF, 10 mL). The solution was stirred in advance for 1 h at ambient temperature. After stirring the mixture for 12 h at ambient temperature, the organic layer was extracted with chloroform and concentrated in vacuum. After purification by column chromatography on silica using hexane as eluent, *n*-butyl-thiosulphonate was collected as light yellow oil. ^1H NMR ($CDCl_3$, 400 MHz): δ 0.89 (t, 6H, CH_3), 1.36 (m, 4H, CH_3CH_2), 1.65 (2H, m, CH_2CH_2S), 1.82 (m, 2H, $CH_2CH_2S(O)_2$), 3.09 (t, 2H, CH_2S), 3.25 (t, 2H, $CH_2S(O)_2$) ppm; IR (KBr): 2960, 2931 ν (CH_2 asymm.), 2873 ν (CH_2 symm.), 1463 ν (CH_2–S deformation), 1324, 1130 ν ($S(O)_2$) cm^{-1}.

3. Results and discussion

The conversion process contains five reaction steps (Scheme 1, I–V). The thermal decomposition of sulphinyl groups bearing a β-hydrogen atom provides a convenient route for the synthesis of olefins [23]. In this reversible elimination reaction, proceeding by the *syn*-intramolecular mechanism, sulphenic acids are produced (I) [24,25]. These sulphenic acids have a very high reactivity, due to the fact that, in the absence of trapping agents, they readily undergo intermolecular dehydration (dimerisation, II) to give thiosulphinates and water [26]. The sulphenic acids, associated by hydrogen bonds, may behave both as S nucleophiles and S electrophiles [27]. The thiosulphinate itself is not thermally stable and yields a thiosulphonate and a disulphide in a disproportionation reaction (III) [28]. This reaction occurs via a radical mechanism with a homolytic splitting of the S(O)–S bond [29]. The formed thienyl radicals dimerise to give the disulphide (III^1) and the sulphinyl radicals dimerise to give thiosulphonate (III^2). Disulphide and thiosulphonate are called as elimination products in this study. In solid state conversion, these

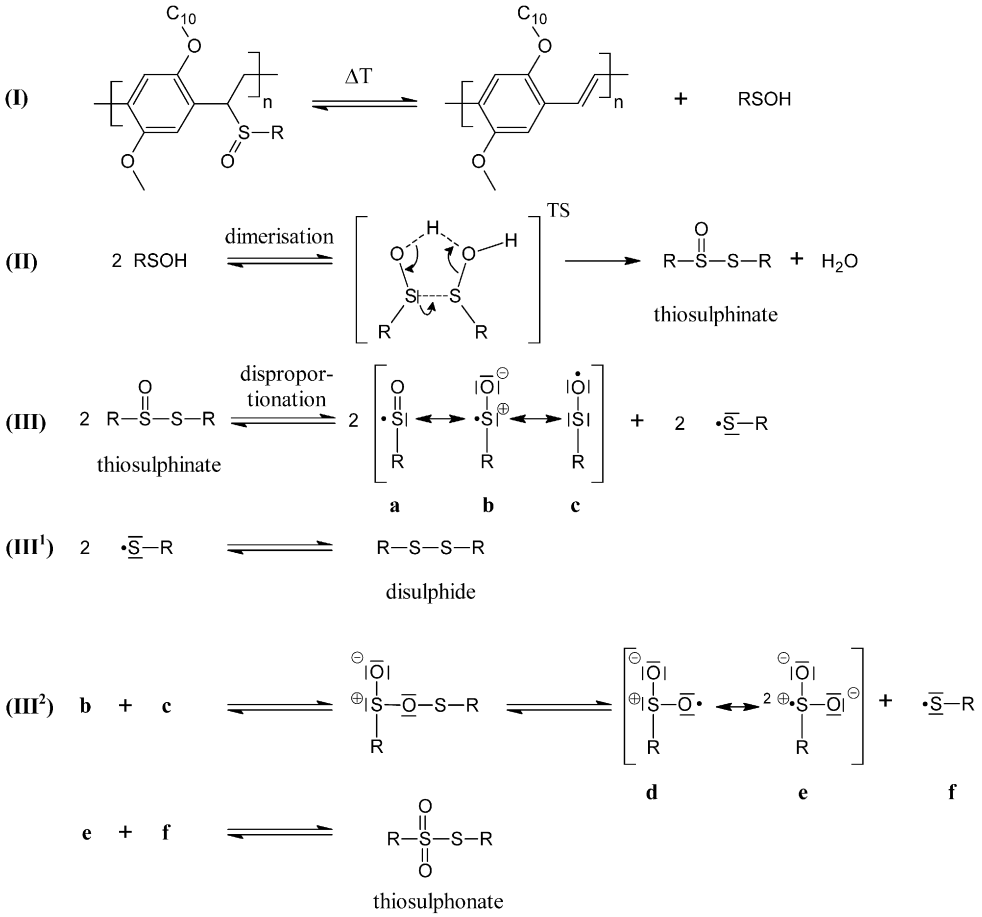

Scheme 1. Mechanism of the conversion process of alkyl sulphinyl PPV precursor polymer to the conjugated OC_1C_{10}-PPV polymer.

elimination products could possibly interact with the conjugated system (network formation) (IV). Once the elimination products are formed, these products have to diffuse and evaporate out of the polymer matrix (V).

The elimination reaction (Scheme 1, I) from precursor polymer towards conjugated material can be followed with in situ FT-IR spectroscopy via the formation of the *trans* vinylene double bond (965 cm^{-1}) as well as by the disappearance of the IR absorbance of the sulphinyl group (1038 cm^{-1}) versus time or temperature. More results concerning the conjugated sequences formed during the thermal conversion can be derived from the UV–vis spectra. However, the focus in this study will by laid on modulated temperature differential scanning calorimetry (MTDSC), which will be applied to evaluate the subsequent reaction steps of the conversion process (Scheme 1, II–IV). MTDSC is an extension of DSC in which the linear rise in temperature is modulated by a small perturbation, in this case a sinusoidal wave adds a new dimension to the conventional approach [30]. In addition to the heat flow signal (non-reversing heat flow, NR), it is also possible to measure the heat capacity (C_p) simultaneously. In this work, water and elimination products that are set free during the dimerisation and disproportionation reactions cause an increase in C_p. Finally, isothermal thermogravimetric analysis (TGA) will be used to study the diffusion and evaporation of the elimination products (Scheme 1, V).

3.1. Thermal elimination reaction of n-alkyl-sulphinyl OC_1C_{10}-PPV precursor polymer studied with in situ FT-IR and UV–vis spectroscopy (Scheme 1, I)

In situ elimination reactions were performed at 2 °C/min up to 250 °C under a continuous flow of nitrogen, for the *n*-butyl- and the *n*-octyl-sulphinyl OC_1C_{10}-PPV precursor polymer. The elimination reaction from precursor to conjugated polymer can be followed via the formation of the *trans* vinylene double bond (at 965 cm^{-1}) and at the same time via the disappearance of the sulphinyl group (at 1038 cm^{-1}). In Fig. 1, the increase of the *trans* vinylene double bond signal and the decrease of the sulphinyl signal as a function of increasing temperature are displayed. The elimination of the *n*-butyl-sulphinyl precursor starts at approximately 70 °C and is completed at approximately 110 °C under these heating conditions. Similar results in elimination behaviour were obtained with the *n*-octyl-sulphinyl as the eliminable group. Above 110 °C the absorbance of the *trans* vinylene double bond (at 965 cm^{-1}) decreases gradually. This is attributed to the thermochromic effect [17]. In the FT-IR spectra no indication towards the formation of the less stable *cis* vinylene double bonds can be found.

A second spectroscopic technique that gives insight into the elimination reaction is in situ UV–vis spectroscopy, by which the formation of the conjugated system itself can be evaluated. During elimination there is a continuous red shift observed. In the first part, oligomeric conjugated fragments are formed, but at a higher extent of elimination the absorption band becomes broad as the full distribution of conjugation lengths develops

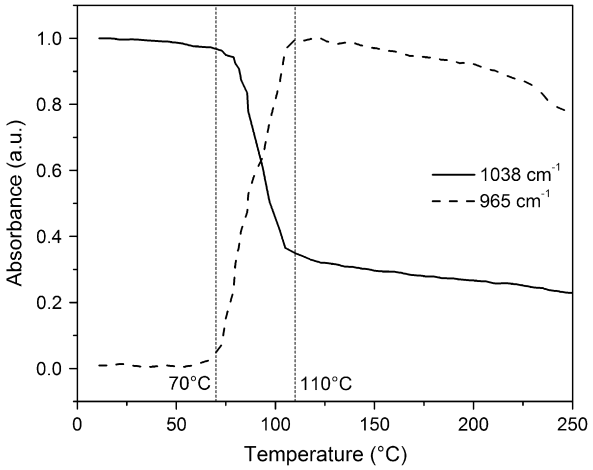

Fig. 1. Evolution of the FT-IR absorbance at 1038 cm^{-1} (sulphinyl group) and 965 cm^{-1} (*trans* C=C) as a function of increasing temperature for the conversion process of *n*-butyl-sulphinyl OC_1C_{10}-PPV precursor polymer.

(Fig. 2). A similar temperature program as that for FT-IR is used (2 °C/min up to 250 °C). The intensity of λ_{max} (=490 nm) as a function of temperature is measured (Fig. 3), showing the formation of the conjugated system in a temperature range from 75 up to 110 °C. The striking similarity with the results obtained with FT-IR demonstrates that both techniques give similar information and indicates that the elimination reaction itself is observed. Above 110 °C the absorbance at 490 nm decreases, however, more markedly than for the FT-IR results. For the UV results, the decrease can again be attributed to the thermochromic effect [17], which leads to a hypsochromic shift of λ_{max}.

3.2. Dimerisation and disproportionation reactions studied with MTDSC (Scheme 1, II, III)

The *n*-butyl-sulphinyl OC_1C_{10}-PPV precursor polymer is heated at 2.5 °C/min from −45 up to 180 °C, followed by a

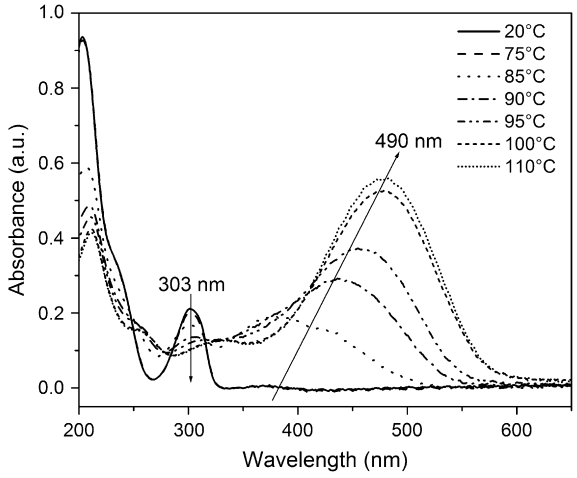

Fig. 2. UV-absorption spectra as a function of increasing temperature for the conversion process of *n*-butyl-sulphinyl OC_1C_{10}-PPV precursor polymer.

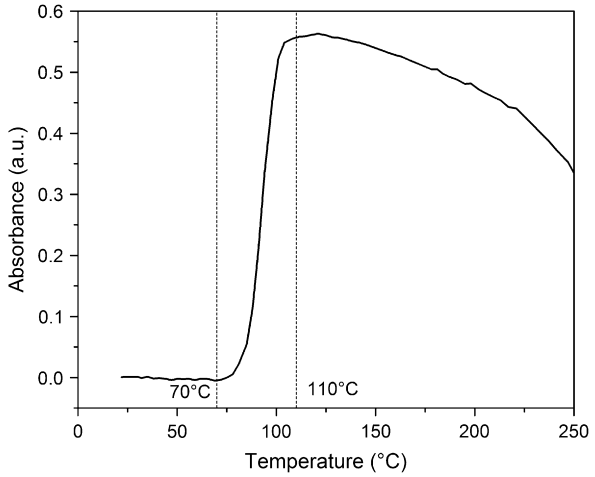

Fig. 3. The UV absorbance at 490 nm (λ_{max} of the conjugated system) as a function of increasing temperature for the conversion process of *n*-butyl-sulphinyl OC_1C_{10}-PPV precursor polymer.

cooling and a second heating at the same rate (Fig. 4). Theoretical calculations of the conversion process demonstrate that the elimination reaction (Scheme 1, I) is an endothermic reaction ($\Delta U = 46.8$ kJ/mol) [31], while the dimerisation (Scheme 1, II) and disproportionation (Scheme 1, III+III^1+III^2) reaction pathways are both exothermic, with ΔU equal to −70.3 and −57.4 kJ/mol, respectively [32–37]. From Fig. 4, it is clear that at around 70 °C no heat effect is visible. Probably, this means that the dimerisation reaction occurs almost simultaneously with the elimination reaction, cancelling out the heat effect of the elimination reaction, and leading to a largely thermoneutral reaction process up to 90 °C.

Fig. 4 also shows that in the first heating run (Fig. 4, (1)) an increase in the C_p-signal is observed in a temperature range at around 36 °C, corresponding to the glass transition temperature (T_g) of the *n*-butyl-sulphinyl OC_1C_{10}-PPV precursor polymer. The T_g of the conjugated OC_1C_{10}-PPV polymer, as measured with a Liquid Nitrogen Cooling Accessory (LNCA) is −62 °C (not visible in Fig. 4). This means that elimination products, formed in situ during the MTDSC experiment, act as plasticizers in the conjugated polymer matrix, causing a significant decrease in T_g. A conjugated OC_1C_{10}-PPV polymer eliminated in toluene (ex situ) contains no elimination products and has a very broad T_g at around 50 °C ranging from 25 to 75 °C. This broad T_g probably arises from the fact that the alkoxy chains act as internal plasticizers and/or relate to the regio-irregular structure of the polymer chain of OC_1C_{10}-PPV.

In the first heating run (Fig. 4, (1)), in the temperature range from 85 up to 170 °C, a large exothermic heat effect of −80.6 J/g is observed in the NR heat flow. Based on a molar mass of 393 g/mol of the repeating unit, this corresponds to −31.8 kJ/mol of repeating unit. In the same temperature range, a second increase in C_p is observed at around 126 °C. This can be attributed to reactions of the elimination products, namely the dimerisation reaction of sulphenic acids and/or the disproportionation reaction of *n*-butyl-thiosulphinate. To confirm this statement and to disentangle the reaction steps in the mechanism (Scheme 1), the latter component was synthesized (see Section 2). The heat capacity signal and non-reversing heat flow signal of non-isothermal experiments on *n*-butyl-sulphinyl OC_1C_{10}-PPV precursor polymer and *n*-butyl-thiosulphinate are shown in Figs. 5 and 6, respectively. The increase in C_p at 126 °C seems to correspond to the disproportionation reaction of the *n*-butyl-thiosulphinate.

In the non-isothermal experiment with pure *n*-butyl-thiosulphinate, a change in heat capacity of 0.24 J/g/°C is seen near 126 °C, while for the *n*-butyl-sulphinyl OC_1C_{10}-PPV precursor polymer a change in heat capacity of 0.20 J/g/°C is measured. The maximum amount of *n*-butyl-thiosulphinate that can be released during the elimination process can be calculated from the reaction equations and equals 24.7%. In other words, the pure *n*-butyl-thiosulphinate could cause an increase in heat

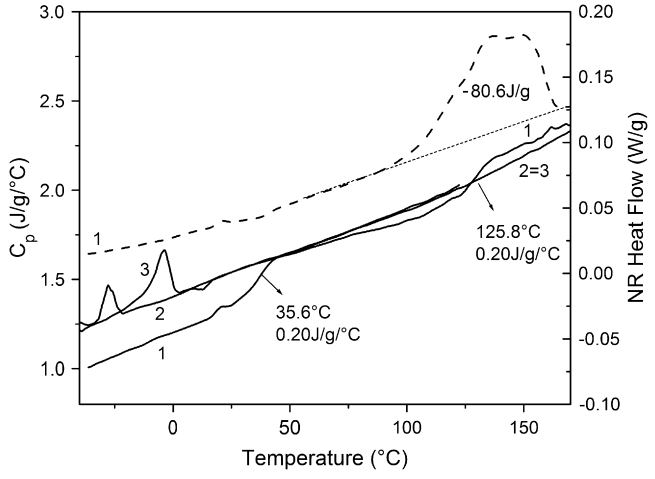

Fig. 4. Heat capacity C_p (solid) and non-reversing (NR) heat flow (dashed) versus temperature from a non-isothermal MTDSC experiment on *n*-butyl-sulphinyl OC_1C_{10}-PPV precursor from −45 up to 180 °C at 2.5 °C/min (1), followed by a cooling (2), and a second heating (3) at the same heating rate. This measurement is carried out in the solid state in a HPS pan.

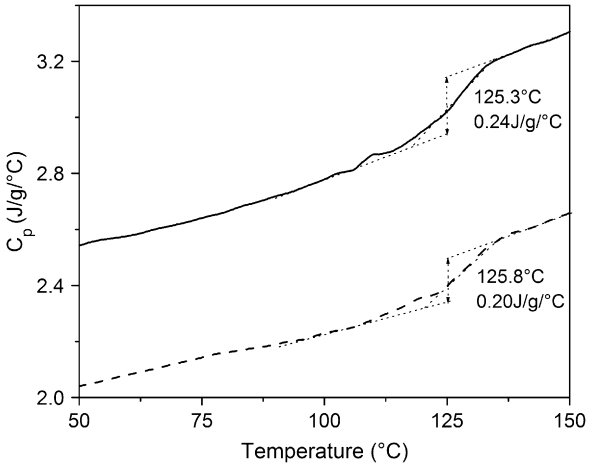

Fig. 5. Heat capacity C_p versus temperature from non-isothermal MTDSC experiments on *n*-butyl-sulphinyl OC_1C_{10}-PPV precursor polymer (dashed) and *n*-butyl-thiosulphinate (solid).

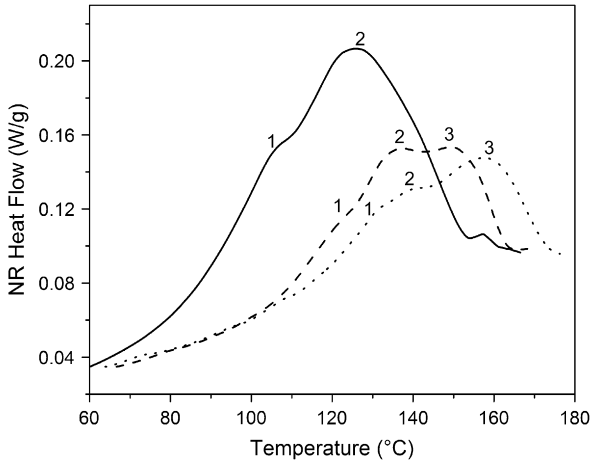

Fig. 6. NR heat flow versus temperature from non-isothermal MTDSC experiments on *n*-alkyl-sulphinyl OC_1C_{10}-PPV precursor polymer (*n*-butyl: dashed, *n*-octyl: dotted) and *n*-butyl-thiosulphinate (solid). The exothermic peaks of the precursor polymers are normalized to the maximum quantity of *n*-butyl-thiosulphinate formed during the elimination process. The subsequent peaks are indicated by numbers.

capacity of around 0.06 J/g/°C (or 0.247 × 0.24 J/g/°C). This is too small to explain the increase in C_p in the measurement of the *n*-butyl-sulphinyl OC_1C_{10}-PPV precursor polymer. Probably, the increase in heat capacity around 126 °C should be attributed to different reactions (ongoing dimerisation and disproportionation) for which the temperature intervals overlap.

In Fig. 6, the exothermic peaks in the NR heat flow signal for the *n*-butyl- and *n*-octyl-sulphinyl OC_1C_{10}-PPV precursor polymers and for pure *n*-butyl-thiosulphinate are compared. The *n*-butyl-sulphinyl OC_1C_{10}-PPV precursor polymer shows three overlapping peaks. On the other hand, the pure *n*-butyl-thiosulphinate shows only two overlapping peaks. The first two exothermic peaks for the precursor polymer are therefore most likely related to the disproportionation reactions (Scheme 1, III). Their shift to a higher temperature can be attributed to a restricted diffusion of thiosulphinate in the polymer matrix.

This can be supported by comparing the elimination of the *n*-butyl- with the *n*-octyl-sulphinyl OC_1C_{10}-PPV precursor polymer (Fig. 6). The shift in the exothermic peak to higher temperature for the latter is probably due to the more restricted diffusion of the elimination products in the polymer matrix for a larger R-group. The third exothermal peak observed for the precursor polymer (3, around 150 °C) is absent during the reaction of thiosulphinate. This indicates an interaction between the OC_1C_{10}-PPV and the elimination products.

3.3. Network formation studied with MTDSC (Scheme 1, IV)

Fig. 5 shows that the increase in heat capacity, originating from the disproportionation reaction, ends at around 135 °C. This means that the exothermic peak that appears above 135 °C in the non-reversing heat flow (Fig. 6) can be attributed to reactions other than the disproportionation reaction. An interaction of the elimination products with the conjugated polymer, causing network formation (crosslinks) is probably occurring. To find evidence for this hypothesis, it was attempted to dissolve the conjugated OC_1C_{10}-PPV polymer, obtained after a non-isothermal measurement up to 200 °C, in $CHCl_3$. The polymer swells in the solvent, but is not soluble anymore. A non-isothermal heating experiment up to 140 °C (just before exothermic peak 3), however, yields a conjugated polymer that is still soluble in $CHCl_3$. This supports network formation in the temperature range of the third exothermic peak in Fig. 6. To investigate the reagents causing this side reaction, a non-isothermal experiment was performed on an already conjugated OC_1C_{10}-PPV polymer (without elimination products) from −45 up to 140 and 200 °C at 2.5 °C/min. In both heating experiments (up to 140 and 200 °C), no significant exothermic signal is present in the NR-signal between 85 and 170 °C (Fig. 7, solid line). Moreover, both polymers remain soluble in $CHCl_3$. Thus, the elimination products are causing network formation. Additional confirmation in this respect can be obtained by adding pre-synthesized elimination products to an already conjugated OC_1C_{10}-PPV polymer. In presence of an excess (>25%) of *n*-butyl-thiosulphinate, a large exothermic signal with three exothermic peaks is visible in the NR heat flow between 85 and 170 °C (Fig. 7, dashed line). After this experiment, the polymer is no longer soluble, which is indicative for network formation. When an excess of *n*-butyl-disulphide and *n*-butyl-thiosulphonate, the end products of the disproportionation reaction, is added to the conjugated OC_1C_{10}-PPV polymer, an exothermic signal in the NR-signal is present with one exothermal peak at 158 °C (Fig. 7, dotted line). It can therefore be concluded that the first two shoulders in the exothermic signal correlate with the dimerisation (partly) and disproportionation reactions, while the last one relates to the occurrence of network formation initiated by the elimination products.

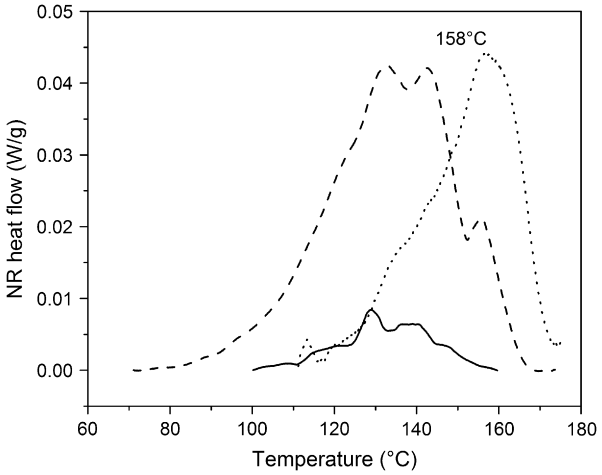

Fig. 7. NR heat flow versus temperature from non-isothermal MTDSC experiments on pure OC_1C_{10}-PPV (solid), OC_1C_{10}-PPV with an excess of *n*-butyl thiosulphinate (dashed), and OC_1C_{10}-PPV with an excess of *n*-butyl-disulphide and thiosulphonate (dotted).

3.4. Diffusion and evaporation of the elimination products studied with TGA (Scheme 1, V)

To ensure an optimal quality for the conjugated polymer film, it is important that all the elimination products can be evaporated from the polymer matrix. As elaborated before, the elimination products lower the T_g of the film, and reactions between the elimination products and the conjugated polymer cause network formation.

To investigate the effect of temperature on the evaporation of the elimination products out of the film, TGA measurements were performed on the *n*-octyl-sulphinyl OC_1C_{10}-PPV precursor polymer at 85 and 100 °C (Fig. 8). The difference in sample weight (film thickness) for the two experiments was minimized. As can be anticipated, a faster evaporation of the elimination products is observed at higher temperatures.

In Fig. 9, isothermal TGA experiments from polymer films with different thickness (0.55 mg: 5.6 μm; 0.73 mg: 7.2 μm; and 2.64 mg: 24.8 μm) are shown at 100 °C. It is clear that the film thickness is very crucial for the evaporation of the elimination products. The thinner the film, the faster the elimination products can diffuse out of the polymer matrix. Note that the film thicknesses used for electronic applications are much smaller (0.01 μm), meaning that the time needed for all elimination products to diffuse out of the polymer matrix will be much shorter.

As discussed in relation to Fig. 6, the diffusion of elimination products depends on the size of the R-group. This also affects the rate with which these products are expelled from the polymer film. Diffusion depends on the molecular weight of the species that will diffuse out of the polymer matrix [2]. This is demonstrated with TGA measurements, carried out on the *n*-ethyl- and *n*-octyl-sulphinyl OC_1C_{10}-PPV precursor polymer (Fig. 10). For the *n*-alkyl-sulphinyl OC_1C_{10}-PPV precursor polymers with an *n*-octyl and *n*-ethyl as R-group, a weight loss of 36 and 21% is calculated from the reaction equation for 100% elimination, respectively. The experimental weight loss for the *n*-ethyl precursor polymers, obtained at

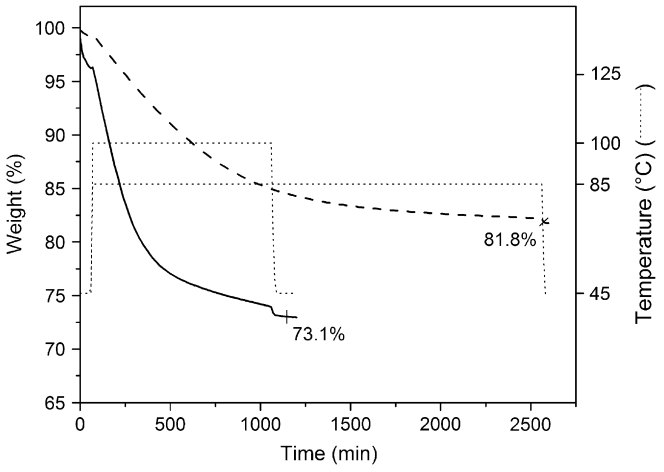

Fig. 8. Sample weight versus time from TGA measurements performed on *n*-octyl-sulphinyl OC_1C_{10}-PPV precursor polymer at 85 °C (dashed) and 100 °C (solid). The temperature profiles are shown as dotted lines.

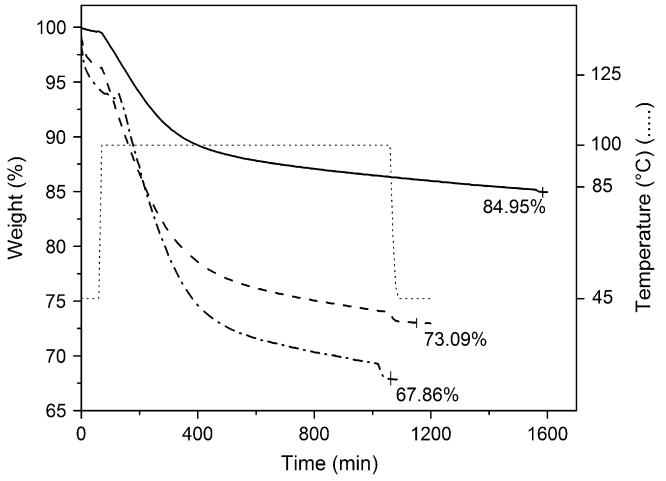

Fig. 9. Sample weight versus time from TGA measurements performed on *n*-octyl-sulphinyl OC_1C_{10}-PPV precursor polymer at 100 °C for different sample weights (different film thicknesses): 2.639 mg (solid); 0.725 mg (dashed); and 0.551 mg (dash-dotted). The temperature profiles are shown as dotted lines.

85 °C after 2500 min (20.9%), is in good agreement with the calculated value. On the other hand, a weight loss of only 17.5% is measured for the *n*-octyl precursor polymer at 85 °C, corresponding to half the calculated weight loss. This indicates that the limited diffusion for the *n*-octyl precursor polymer restricts the evaporation of the elimination products. Additional temperature steps are considered in Fig. 10 to determine the maximum weight loss. The final weight loss for the *n*-ethyl-sulphinyl OC_1C_{10}-PPV precursor polymer (at 200 °C: 26%) cannot be attributed to the evaporation of the elimination products alone, indicating the occurrence of degradation. For the *n*-octyl-sulphinyl OC_1C_{10}-PPV precursor polymer a maximum weight loss of 30% is found, which is still lower than the calculated value. As stated before, much thinner polymer films are used in practice, which means that the evaporation of elimination products occurs much faster.

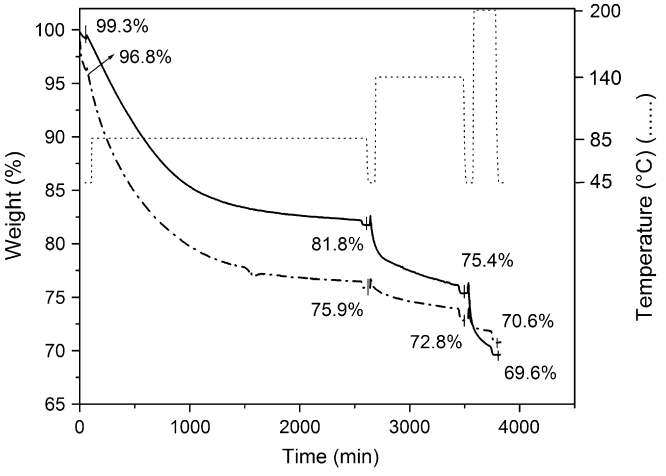

Fig. 10. Sample weight versus time from TGA measurements performed on *n*-alkyl-sulphinyl OC_1C_{10}-PPV precursor polymers with two different R-groups: *n*-octyl (solid) and *n*-ethyl (dashed). The temperature profiles are shown as dotted lines.

Nevertheless, vacuum conditions should be considered for an easier and better evaporation of the elimination products to avoid deterioration of final film quality.

4. Conclusions

The conversion process of *n*-alkyl-sulphinyl OC_1C_{10}-PPV precursor polymers is characterized by five different steps as depicted in Scheme 1. While FT-IR and UV–vis spectroscopy can be used to study the formation of the conjugated system in the elimination reaction, MTDSC is a good technique to study the subsequent reactions (dimerisation, disproportionation and network formation). In the non-isothermal MTDSC experiments, no heat effect is visible for the elimination reaction itself. This indicates that the dimerisation reaction spontaneously follows the elimination reaction. Subsequently, the disproportionation reaction happens in a temperature range between 85 and 135 °C. Both reactions are observed as an increase in C_p.

The elimination products formed can interact with the conjugated polymer and cause network formation, deteriorating the film quality. This effect is seen as an exothermic peak in the NR heat flow with a maximum at around 160 °C. To avoid this side reaction, evaporation of the elimination products out of the film should be promoted. TGA experiments show that the diffusion and evaporation of the elimination products out of the polymer matrix can be accelerated by using a smaller R-group, a higher isothermal temperature, and a thinner film. Network formation can also be avoided by performing the elimination at sufficiently low temperatures (<120 °C) and by using vacuum conditions. To limit such side reactions on conversion in solution, build-up of the concentration of the elimination products should be avoided.

Acknowledgments

The Institute for the Promotion of Innovation by Science and Technology in Flanders (IWT) is acknowledged for the Ph.D. grant for E. Kesters. The Inter University Attraction Pole (IUAP) supported by the Belgian Government and the Research Foundation – Flanders (FWO – Vlaanderen) and BOF-UHasselt are acknowledged for financial support. The work of S. Swier was supported by grants of the IWT. G. Van Assche is a Postdoctoral Fellow of the Research Foundation – Flanders (FWO – Vlaanderen).

References

[1] Wessling RA. J Polym Sci Polym Symp 1985;72:55–66.
[2] Braun D, Heeger AJ. Appl Phys Lett 1991;58:1982–4.
[3] Staring EGJ, Demandt RCJE, Braun D, Rikken GLJ, Kessner YARR, Venhuizen THJ, et al. Adv Mater 1994;6:934–7.
[4] Lee JK, Schrock RR, Baigent DR, Friend RH. Macromolecules 1995;28:1966–71.
[5] Hilberer A, Brouwer HJ, van der Scheer BJ, Wildeman J, Hadziioannou G. Macromolecules 1995;28:4525–9.
[6] Kim DU, Tsutsui T, Saito S. Chem Lett 1995;7:587–8.
[7] Gilch HG, Wheelwright WL. J Polym Sci Part A Polym Chem 1966;4:1337.
[8] Louwet F, Vanderzande D, Gelan J. Synth Met 1992;52:125–30.
[9] Louwet F, Vanderzande D, Gelan J, Mullens J. Macromolecules 1995;28:1330–1.
[10] Louwet F, Vanderzande D, Gelan J. Synth Met 1995;69:509–10.
[11] Issaris A, Vanderzande D, Gelan J. Polymer 1995;38(10):2571–4.
[12] Kim ST, Hwang DH, Li XC, Grüner J, Friend RH, Holmes AB, et al. Adv Mater 1996;8(12):979–82.
[13] Gelinck GH, Warman JM, Staring EGJ. J Phys Chem 1996;100(13):5485–91.
[14] Brabec CJ, Sariciftci NS, Hummelen JC. Adv Funct Mater 2001;11(1):15.
[15] van der Ent L. Kunststof Mag 2001;April 3:38.
[16] Munters T, Martens T, Goris L, Vrindts V, Manca J, Lutsen L, et al. Thin Solid Films 2002;403:247–51.
[17] Kesters E, Vanderzande D, Lutsen L, Penxten H, Carleer R. Macromolecules 2005;38:1141–7.
[18] Roex H, Adriaensens P, Vanderzande D, Gelan J. Macromolecules 2003;36:5613–22.
[19] Gaur U, Wunderlich B. J Phys Chem Ref Data 1982;11(2):313–25.
[20] (a) van Breemen A. Ph.D. thesis. Limburgs Universitair Centrum, Diepenbeek; 1999.
(b) Lutsen L, van Breemen AJ, Kreuder W, Vanderzande DJM, Gelan JMJV. Helv Chim Acta 2000;83:3113.
[21] Kondo K, Negishi A, Ojima I. J Am Chem Soc 1972;94(16):5786.
[22] Buter J, Kellogg RM. J Org Chem 1977;42(6):973–6.
[23] Kingsburry CA, Cram DJ. J Am Chem Soc 1960;82:1810.
[24] Shelton JR, Davis KE. Int J Sulphur Chem 1973;8:205.
[25] Cooper RDG. J Am Chem Soc 1970;92:5010.
[26] Trost BM, Leung KK. Tetrahedron Lett 1975;48:4197–200.
[27] Block E, O'Connor J. J Am Chem Soc 1974;96(12):3929–44.
[28] Koch P, Ciuffarin E, Fava A. J Am Chem Soc 1970;92:5971.
[29] Barnard D. J Am Chem Soc 1957;4675.
[30] Reading M, Hourston DJ. Modulated-temperature differential scanning calorimetry: theoretical and practical applications in polymer characterisation (hot topics in thermal analysis and calorimetry). UK: Springer; 2006.
[31] Kwasniewski SP, François JP, Deleuze MS. Int J Quantum Chem 2001;85:557–68.
[32] Kwasniewski SP, François JP, Deleuze MS. J Phys Chem A 2003;107:5168–80.
[33] Claes L, Francois JP, Deleuze MS. J Am Chem Soc 2002;124(25):7563–72.
[34] The geometries of the stationary points (reactant and product) identified along the dimerisation (Scheme 1, II) and disproportionation (Scheme 1, III–III^2) reaction pathways have been fully optimized using Density Functional theory [35] along with the MPW1K (modified Perdew–Wang 1-parameter model for kinetics) [36,37] functional in conjunction with the 6-311G** basis set [38,39]. The performance of the MPW1K/6-311G** method has been specifically assessed for the conversion of sulphoxide precursors into model oligomers of conjugated polymers such as PPV [33]. The internal reaction energies (ΔU), presented here are differences of total electronic energies, without zero-point vibrational energies (personal communication, Claes L, Francois JP, Deleuze MS. Universiteit Hasselt, Belgium).
[35] Parr RG, Yang W. Density functional theory of atoms and molecules. Oxford: Oxford University Press; 1993.
[36] Lynch BJ, Fast PL, Harris M, Truhlar DG. J Phys Chem A 2000;104(21):4811–5.
[37] Lynch BJ, Truhlar DG. J Phys Chem A 2001;105(13):2936–41.
[38] Krishnan R, Binkley JS, Seeger R, Pople JA. J Chem Phys 1980;72(1):650–4.
[39] McLean AD, Chandler GS. J Chem Phys 1980;72(10):5639–48.